

# COMPASS: Navigating Global Marine Lead Data Integration through Expert-Guided LLM Agent

Yiming Liu

School of Information Science and Electronic Engineering,  
Shanghai Jiao Tong University  
Shanghai, China  
liu-ym@sjtu.edu.cn

Bin Lu\*

School of Information Science and Electronic Engineering,  
Shanghai Jiao Tong University  
Shanghai, China  
robinlu1209@sjtu.edu.cn

Meng Jin\*

School of Artificial Intelligence,  
Shanghai Jiao Tong University  
Shanghai, China  
jinm@sjtu.edu.cn

Ziyuan Sang

School of Information Science and Electronic Engineering,  
Shanghai Jiao Tong University  
Shanghai, China  
sangziyuan@sjtu.edu.cn

Shuo Jiang

State Key Laboratory of Estuarine and Coastal Research,  
East China Normal University  
Shanghai, China  
jiangshuo@sklec.ecnu.edu.cn

Lei Zhou

School of Oceanography,  
Shanghai Jiao Tong University  
Shanghai, China  
zhoulei1588@sjtu.edu.cn

Xinbing Wang

School of Information Science and Electronic Engineering,  
Shanghai Jiao Tong University  
Shanghai, China  
xwang8@sjtu.edu.cn

Chenghu Zhou

Institute of Geographical Science and Natural Resources Research,  
Chinese Academy of Sciences  
Beijing, China  
zhouch@reis.ac.cn

Jing Zhang

State Key Laboratory of Estuarine and Coastal Research,  
East China Normal University  
Shanghai, China  
jzhang@sklec.ecnu.edu.cn

## Abstract

Marine lead (Pb) and its isotopes are critical tracers for ocean circulation and anthropogenic pollution, yet in-situ observations remain costly and sparse. While vast historical records exist, they lie buried within the unstructured content of academic papers, creating “data silos” inaccessible to comprehensive analysis. Manual extraction is unscalable, while general-purpose Large Language Models (LLMs) lack the necessary domain-specific knowledge, leading to hallucinations and scientifically invalid outputs. To address this, we introduce an expert-guided adaptation approach that enables LLMs to perform rigorous scientific data extraction without fine-tuning. We operationalize this approach through COMPASS, an LLM agent framework enhanced by a Knowledge Tree co-designed with marine scientists, which decomposes complex tasks into verifiable steps, guiding the agent’s reasoning to ensure scientific validity. Deploying COMPASS across a corpus of over 230,000 relevant open-access papers, we successfully extract 3,751 *previously unincorporated Pb records*. This effort establishes the largest integrated marine Pb database to date. Beyond standard metrics, COMPASS demonstrates superior reliability through multi-layered validation, achieving 92% accuracy as confirmed through expert manual verification. The newly integrated data expand coverage in previously under-sampled regions

\*Bin Lu and Meng Jin are co-corresponding authors.

such as the East China Sea and the Southern Ocean, providing an enriched data foundation for future scientific discoveries. We release an interactive visualization platform<sup>1</sup> to facilitate open scientific access. Our work demonstrates that expert-guided agents can effectively bridge the gap between general-purpose LLMs and high-stakes scientific domains, enabling scalable data discovery in geosciences.<sup>2</sup>

## CCS Concepts

• **Computing methodologies** → **Information extraction; Knowledge representation and reasoning**; • **Information systems** → **Mediators and data integration**; • **Applied computing** → **Earth and atmospheric sciences**.

## Keywords

Scientific Data Integration; LLM Agent; Knowledge Tree; Marine Geochemistry; AI for Science

## ACM Reference Format:

Yiming Liu, Bin Lu, Meng Jin, Ziyuan Sang, Shuo Jiang, Lei Zhou, Xinbing Wang, Chenghu Zhou, and Jing Zhang. 2026. COMPASS: Navigating Global Marine Lead Data Integration through Expert-Guided LLM Agent. In *Proceedings of the 32nd ACM SIGKDD Conference on Knowledge Discovery and Data Mining V.2 (KDD '26)*, August 09–13, 2026, Jeju Island, Republic of Korea. ACM, New York, NY, USA, 12 pages. <https://doi.org/10.1145/3770855.3819001>

## 1 Introduction

Trace elements and their isotopes (TEIs) in the ocean serve as vital diagnostic tools for deciphering Earth system dynamics. Among

<sup>1</sup>Please visit our online platform at <https://jingwei.acemap.cn/lead>.

<sup>2</sup>Our code is available at <https://github.com/liuyiming01/COMPASS>.



This work is licensed under a Creative Commons Attribution 4.0 International License. *KDD '26, Jeju Island, Republic of Korea*

© 2026 Copyright held by the owner/author(s).

ACM ISBN 979-8-4007-2259-2/2026/08

<https://doi.org/10.1145/3770855.3819001>

them, lead (Pb) and its isotopes are particularly important, functioning as powerful tracers for ocean circulation pathways and anthropogenic pollution history [7, 18]. Since Patterson’s seminal work [33] revealed global industrial Pb contamination, marine Pb has been extensively monitored to capture the temporal evolution of anthropogenic emissions.

However, the inherent scarcity of high-quality marine Pb data creates a significant bottleneck for global-scale analysis. Obtaining these records requires expensive oceanographic cruises and strict trace-metal-clean protocols [15, 44], making every data point a high-value asset. While a substantial volume of historical in-situ observations has accumulated over decades, the vast majority remain buried within the unstructured text, tables, and figures of academic papers. This phenomenon has created a “data silo” problem, where critical datasets are scattered and effectively unavailable for global-scale synthesis.

**Prior works.** Existing efforts to bridge this gap have primarily relied on two integration paradigms: manual curation and automated extraction. Manual curation, exemplified by the GEOTRACES program [3] and analogous synthesis efforts across paleobiology [12] and terrestrial biogeochemistry [1, 27], ensures high data fidelity but is labor-intensive and unscalable against the exponential growth of literature. Conversely, automated approaches—spanning discriminative models [5], domain-specific LLMs [6, 11], multimodal document parsing [37, 45], and retrieval-augmented generation (RAG) [24, 26]—offer scalability but often treat scientific extraction as a probabilistic text task. Lacking domain-specific logical constraints, these methods frequently misinterpret fine-grained details—such as isotope notations or unit conversions—resulting in hallucinations that compromise scientific validity.

**Challenges.** To achieve both scalability and scientific rigor, effective automation requires addressing two fundamental barriers: (1) *The Domain Knowledge Gap*: General-purpose LLMs lack the specialized knowledge and strict logical constraints required for scientific research. Without domain-specific guidance, these models often hallucinate or fail to distinguish between subtle scientific nuances, rendering their outputs unreliable for high-stakes analysis. (2) *Structural Heterogeneity*: Scientific records are deeply embedded within unstructured text and diverse table formats. Extracting this fine-grained data requires a sophisticated, systematic workflow capable of navigating these complex structures, rather than simple information retrieval.

**Our Work.** To address these challenges, we propose COMPASS, a Knowledge Tree-enhanced LLM Agent framework designed to operationalize an expert-guided adaptation. Instead of relying on black-box fine-tuning, COMPASS adopts an *expert-in-the-loop* philosophy. We co-designed a domain-specific Knowledge Tree with marine scientists, encoding rigorous reasoning logic to guide the automated process. Leveraging this structured guidance, COMPASS decomposes the integration task into hierarchical subtasks across three phases—collection, extraction, and aggregation—with validation checks embedded at each step to ensure that every extracted record satisfies physical constraints. By deploying COMPASS on over 230,000 relevant open-access papers, we successfully recovered 3,751 previously unincorporated Pb records, demonstrating the framework’s capability to bridge the gap between everyday

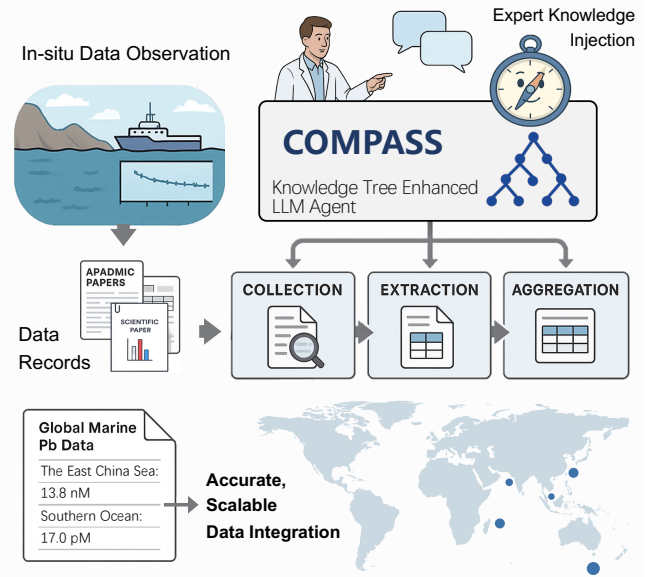


**Figure 1: Overview of the COMPASS framework for marine Pb data integration.**

language models and rigorous scientific demands. The main contributions of this work are summarized as follows:

- We develop COMPASS, a Knowledge Tree-enhanced LLM Agent framework that hierarchically decomposes complex scientific workflows, enabling accurate extraction and integration of fine-grained data (text and tables) from heterogeneous academic sources.
- We demonstrate that expert-guided knowledge injection via a co-designed Knowledge Tree can effectively bridge the gap between general-purpose LLMs and high-stakes scientific domains without fine-tuning, providing a practical and low-cost alternative to domain-specific model training.
- We deploy COMPASS to establish the largest integrated marine Pb database to date, recovering 3,751 previously unincorporated records from over 230,000 open-access papers. The integrated data substantially expand coverage in under-sampled regions such as the East China Sea and the Southern Ocean, providing an enriched data foundation for future scientific discoveries.

## 2 Related Work

### 2.1 Scientific Data Integration

Integrating heterogeneous scientific data is a cornerstone of data-driven discovery. Existing approaches fall into two paradigms. (1) *Manual Integration*. Research programs such as GEOTRACES [3] and regional syntheses [46] enable systematic integration of marine trace element data through international collaboration. Fan et al. [12] manually synthesize data from thousands of marine fossil species to generate high-resolution biodiversity curves. Similar efforts in terrestrial biogeochemical cycles [1, 27, 28] yield important insights but require substantial human effort, becoming

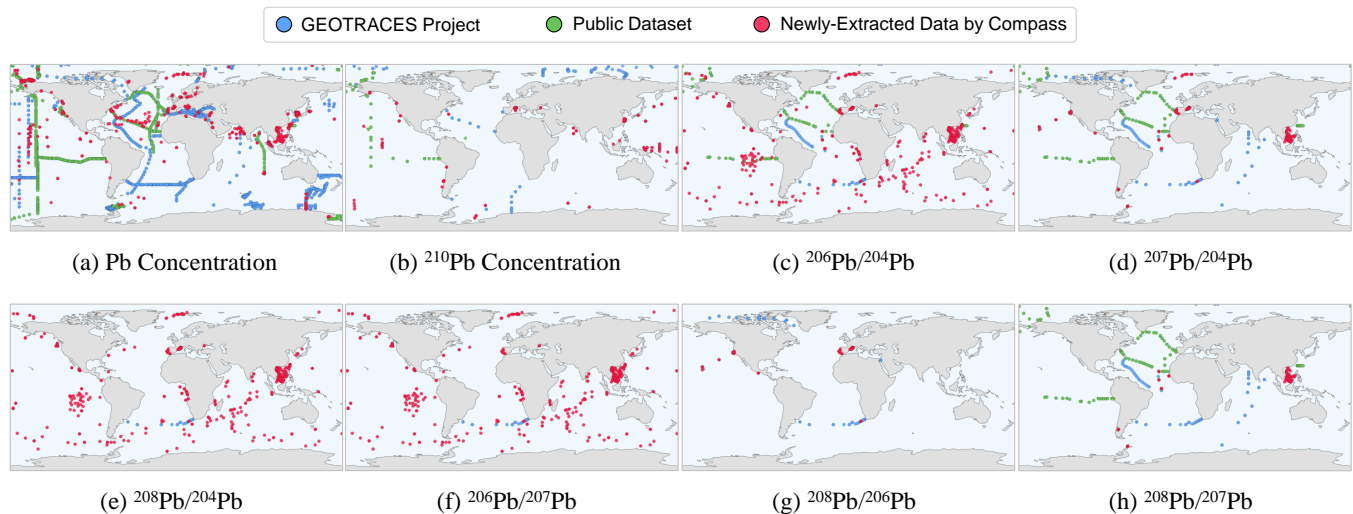


**Figure 2: Global distribution of integrated marine Pb data showing improved coverage across different ocean regions. The eight panels represent different Pb measurements: (a) Pb concentration, (b)  $^{210}\text{Pb}$  concentration, and (c-h) six Pb isotope ratios. The map displays a total of 35,563 marine Pb records, including data extracted by COMPASS and from existing datasets, with color coding indicating data sources.**

increasingly impractical with the exponential growth of publications. (2) *Automated Integration*. Text-based extraction methods have evolved from discriminative models like SciBERT [5] to structured extraction with domain-specific and multi-expert language models [10, 16, 40]. Cross-modality frameworks such as TabPedia [45], MinerU [37], MatViX [22], and Uni-SMART [8] extend beyond text to support joint analysis of tables and figures, with applications spanning document extraction to clinical and materials science data integration [4, 29]. Despite this progress, existing automated methods primarily focus on information extraction from individual documents rather than end-to-end scientific synthesis with physical constraint validation.

## 2.2 Scientific LLM Agents

LLM agents leverage advanced comprehension and reasoning to automate scientific workflows. (1) *Training-based Agents*. Domain-specific LLMs such as K2 [11] for geoscience and OceanGPT [6] for ocean science improve domain knowledge through curated corpora and supervised training. Agent frameworks further employ curriculum learning and reinforcement learning—for example, AutoWebGLM [23] integrates both to improve web navigation for scientific tasks. Multi-agent strategies [13, 17, 21, 38, 42, 43] enable large-scale coordination across domains but typically demand significant computational resources and domain-specific datasets. (2) *Prompting and Retrieval-based Agents*. PaperQA [24] employs retrieval-augmented generation (RAG) to perform evidence-based information retrieval across scientific articles. ChemAgent [35] and SciAgents [14] leverage tool-use and ontological knowledge graphs for multi-agent reasoning, while other approaches explore

self-updating mechanisms and automated environment generation [19, 30]. However, standard RAG or general agents lack structured domain logic for fine-grained integration in high-stakes scientific fields. COMPASS addresses this gap through an expert-guided adaptation approach: instead of probability-based retrieval or costly fine-tuning, it embeds structured expert knowledge directly into the agent’s workflow, ensuring scientific validity while maintaining scalability.

## 3 Background and Problem Formulation

### 3.1 Scientific Significance of Marine Lead

Marine lead (Pb) and its isotopes serve as critical tracers for ocean circulation pathways and anthropogenic pollution history [7, 18]. Pb primarily originates from anthropogenic activities such as leaded gasoline combustion and industrial emissions [31], dispersing via atmospheric transport to even remote ocean regions [9] (Figure 3). Its relatively brief oceanic residence time compared to global mixing timescales enables Pb to retain distinct regional isotopic fingerprints that record transient environmental changes [34, 41], while obtaining high-quality measurements requires expensive oceanographic cruises and strict trace-metal-clean protocols [15, 44].

However, individual studies provide only geographically limited snapshots. A comprehensive integrated database unlocks analyses no single study can achieve: global Pb inventory and distribution estimation, source identification via stable isotope ratios (e.g.,  $^{206}\text{Pb}/^{207}\text{Pb}$ ,  $^{208}\text{Pb}/^{206}\text{Pb}$ ), and investigation of oceanic responses to the global phase-out of leaded gasoline. Multi-decadal observations, when unified, further support biogeochemical modeling and environmental policy evaluation. Despite this potential, vast historical data remain fragmented across decades of publications. Manual curation programs like GEOTRACES [3] and regional syntheses [46]

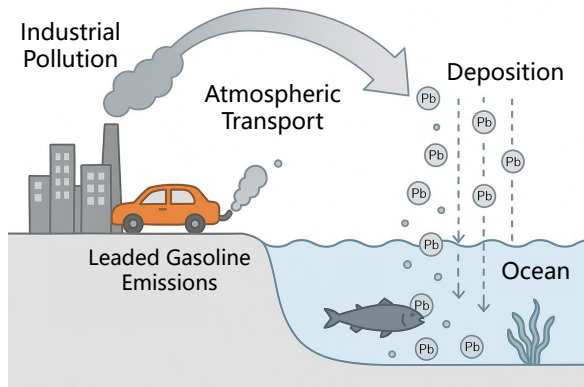


**Figure 3: Pb from anthropogenic emissions enters the ocean through atmospheric transport and surface deposition.**

are fundamentally unscalable, directly motivating the integration framework presented in this work.

### 3.2 The Data Integration Challenge

**Data Source Categorization.** Marine Pb data exists across three categories: *structured databases* ( $\mathcal{D}_{structured}$ ) such as GEOTRACES [3] with well-defined schemas; *scattered datasets* ( $\mathcal{D}_{scattered}$ ) from individual studies with varying conventions; and *academic papers* ( $\mathcal{D}_{papers}$ ), where fine-grained measurements are embedded in unstructured text and diverse table formats.

**Technical Challenges.** While the general challenges of domain knowledge gap and structural heterogeneity apply broadly, marine Pb data integration presents additional domain-specific difficulties: (1) *Data Source Proliferation*: Pb measurements scatter across literature spanning over five decades, making manual integration impractical. (2) *Fine-grained Semantic Complexity*: Subtle distinctions—such as dissolved versus particulate phases, different isotope ratio conventions, and varied analytical methods—are easily confused by general-purpose models. (3) *Cross-source Harmonization*: Inconsistent units, depth references, and coordinate formats demand systematic normalization.

**Problem Formulation.** Each source exhibits distinct schema structures, semantic conventions, and quality standards (e.g., varying units, precision levels, and coordinate formats), necessitating a hierarchical pipeline that progressively resolves these heterogeneities. We formalize the data integration objective as constructing a unified dataset  $\mathcal{D}^*$  from heterogeneous sources  $\mathcal{D} = \{D_1, D_2, \dots, D_n\}$  through a hierarchical processing pipeline:

$$\mathcal{D}^* = \mathcal{A}(\mathcal{E}(C(\mathcal{D}_{papers})), \mathcal{D}_{structured}, \mathcal{D}_{scattered}), \quad (1)$$

where  $C$  denotes the collection function that identifies relevant papers from a large candidate corpus,  $\mathcal{E}$  denotes the extraction function that resolves schema heterogeneity and retrieves structured records from paper tables, and  $\mathcal{A}$  denotes the aggregation function that integrates all sources with standardized units, formats, and quality controls.  $\mathcal{D}_{papers} \subset \mathcal{D}$ ,  $\mathcal{D}_{structured} \subset \mathcal{D}$ , and  $\mathcal{D}_{scattered} \subset \mathcal{D}$  represent the academic paper sources, structured database sources, and scattered dataset sources, respectively. This

formulation directly motivates the three-phase architecture of COMPASS.

## 4 COMPASS Framework

### 4.1 Expert-Guided Adaptation Paradigm

Applying LLMs to scientific data integration requires bridging the gap between general-purpose language understanding and rigorous domain reasoning. Existing strategies each have fundamental limitations for this goal. *Fine-tuning* [6, 11] improves domain knowledge but incurs high computational cost and often degrades the instruction-following capabilities critical for multi-step workflows. *Retrieval-Augmented Generation (RAG)* [26] injects knowledge at inference time but treats it as unstructured text fragments, lacking mechanisms to enforce logical constraints or sequential validation across complex pipelines. *Knowledge graph (KG) and ontology-based approaches* [14] organize domain concepts and semantic relationships, but primarily capture declarative knowledge (*what is*) rather than procedural knowledge (*how to act*).

COMPASS introduces an *expert-guided adaptation paradigm* that encodes domain expertise as a structured, executable Knowledge Tree co-designed with domain scientists. Unlike the above approaches, the Knowledge Tree integrates operational logic—prescribing not only *what* the agent should know but also *how* it should reason and validate its outputs—making the workflow interpretable, controllable, and scientifically trustworthy.

### 4.2 Knowledge Tree: Design and Construction

**Definition (Knowledge Tree).** A Knowledge Tree  $T = (N, H, K)$  is a hierarchical structure where  $N$  represents the set of nodes corresponding to specific tasks or subtasks,  $H$  denotes directed edges representing parent-child decomposition relationships, and  $K$  contains expert-provided knowledge constraints associated with each node. Each node  $n_{i,j} \in N$  at level  $L_i$  corresponds to subtask  $t_{i,j}$  and can be decomposed into child nodes at level  $L_{i+1}$ , with leaf nodes representing atomic tasks requiring direct execution.

**Knowledge Structure.** For each node  $n_{i,j}$ , the associated knowledge  $K_{i,j} = \{BK, LC, OG, VC\}$  encompasses four complementary dimensions:

- *Background Knowledge (BK)*: Domain concepts, terminology, and contextual information providing foundational understanding for task execution.
- *Logical Constraints (LC)*: Explicit rules, conditional dependencies, and logical requirements defining valid execution paths.
- *Operational Guidelines (OG)*: Step-by-step procedures, decision heuristics, and output format specifications ensuring standardized execution.
- *Validation Criteria (VC)*: Quality metrics, physical constraint checks, and verification steps enabling automated assessment of output correctness.

This four-dimensional structure ensures that each node carries not only declarative knowledge but also procedural and evaluative guidance, distinguishing our approach from flat structured prompting or static ontologies.

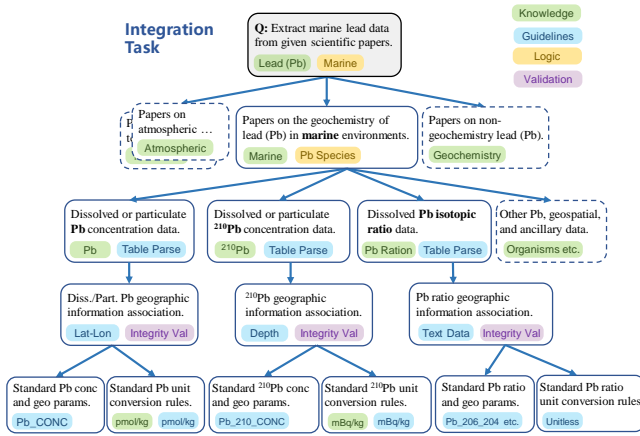


**Figure 4: Domain Knowledge Tree for marine Pb data integration, co-designed by AI researchers and marine scientists.**

**Construction Protocol.** The Knowledge Tree is constructed offline by AI researchers in collaboration with domain experts, following a four-step protocol for each hierarchical level  $L_i$ :

- (1) *Task Context Initialization:* AI researchers present each sub-task along with its hierarchical dependencies, providing domain experts with comprehensive understanding of the task scope and requirements.
- (2) *Expert Knowledge Elicitation:* Domain experts provide specialized knowledge across the four dimensions ( $BK$ ,  $LC$ ,  $OG$ ,  $VC$ ) based on their domain expertise and practical experience.
- (3) *Knowledge Structuring:* AI researchers organize expert-provided knowledge into structured knowledge nodes, ensuring consistency for subsequent automated processing.
- (4) *Completeness Validation:* Domain experts review the constructed knowledge structure for comprehensive coverage of domain requirements before proceeding to the next level.

This four-step protocol is applied iteratively for each hierarchical level, with successive rounds refining the knowledge structure based on expert feedback and agent execution results on representative samples. The finalized Knowledge Tree is then integrated into COMPASS to guide agent deployment.

### 4.3 Marine Pb Knowledge Tree

We collaborate with marine scientists to construct the Knowledge Tree for marine Pb data integration. Figure 4 shows the resulting structure. The overall task is decomposed into hierarchical sub-tasks, with Pb-related papers classified into fine-grained categories for accurate identification. Marine Pb data encompasses multiple types—including Pb concentrations (dissolved, particulate),  $^{210}\text{Pb}$  activity concentrations, and six Pb isotope ratios—each requiring specific data formats, transformation logic, and validation standards. For each subproblem, marine scientists provide the corresponding  $BK$ ,  $LC$ ,  $OG$ , and  $VC$  knowledge.

In practice, the Knowledge Tree construction is a one-time effort: the marine Pb tree (approximately 20 nodes) was built in 6–7 hours by two marine scientists in collaboration with AI researchers.

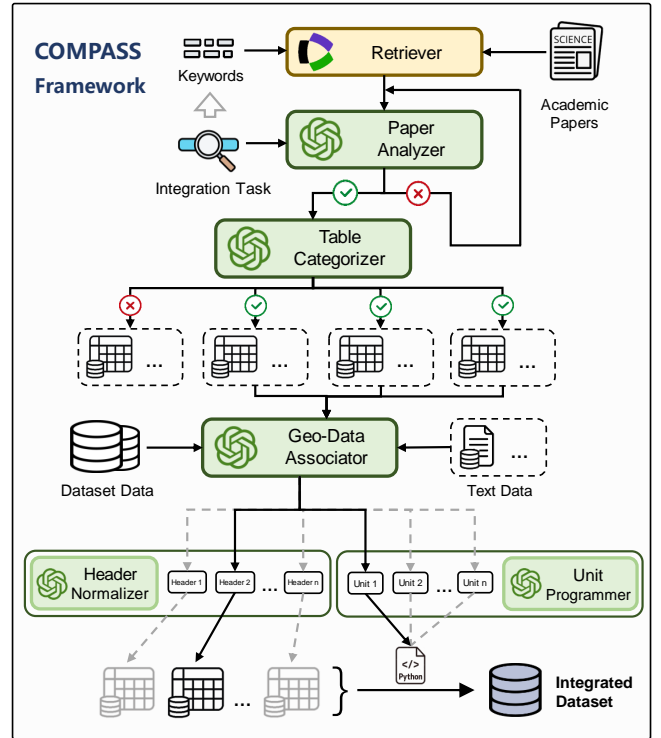


**Figure 5: Architecture of COMPASS: hierarchical agent components and their interactions. (top-down view)**

### 4.4 Agent Deployment

When LLMs directly process complex data integration tasks, they often produce incomplete execution and logical inconsistencies, struggling to maintain coherent reasoning across interdependent subtasks. Inspired by the analytic hierarchy process [36] and hierarchical decision trees [20], COMPASS systematically decomposes complex tasks into a three-phase hierarchical pipeline with five specialized components, as shown in Figure 5.

(1) **Collection Phase.** The *paper classification* component retrieves candidate papers from academic repositories (e.g., Semantic Scholar [2], AceMap [39]) via keyword search, then applies LLM-powered semantic analysis guided by the Knowledge Tree to identify papers containing target data.

(2) **Extraction Phase.** The *table classification* component integrates the PDF parsing tool MinerU [37] to extract tabular content, then leverages LLMs to analyze tables with contextual information (captions, in-text descriptions) to classify and filter target data tables.

(3) **Aggregation Phase.** Three components handle different integration aspects: the *data association* component links related elements within papers (e.g., matching Pb measurements with sampling coordinates from separate tables); the *cross-source fusion* component normalizes heterogeneous table headers into a unified schema; and the *data standardization* component converts values into consistent units through LLM-generated conversion functions.

For each component, the corresponding Knowledge Tree node  $K_{i,j}$  is translated into a domain-aware prompt that systematically

integrates all four knowledge dimensions (*BK, LC, OG, VC*); the complete prompts are publicly available in our GitHub repository, ensuring that the LLM operates with domain-specific context, constrained reasoning boundaries, standardized output formats, and built-in quality checks. A record of completed subtasks and their outputs is maintained across hierarchical levels to preserve consistency. While this study focuses on text and tables, the modular architecture is designed to accommodate additional tools as supplementary components in future extensions. Formally, COMPASS operates as a state transition system where each completed subtask represents a distinct state, with transitions governed by the corresponding Knowledge Tree constraints, ensuring that domain expertise directs every decision point while maintaining systematic progression through the task hierarchy.

#### 4.5 Validation Mechanism

Scientific data integration demands rigorous quality assurance. COMPASS implements a multi-layered validation mechanism informed by the Validation Criteria (*VC*) in the Knowledge Tree.

**Automated Physical Constraint Checks.** Every extracted record undergoes value range verification against physically plausible bounds for each data type, unit conversion cross-validation, and geographical outlier filtering against ocean boundary definitions. When validation failures are detected, COMPASS rolls back the current step and re-processes the failed subtask, preventing error propagation to downstream components.

**Expert Manual Validation.** Beyond automated checks, we conduct manual validation with marine scientists on a randomly selected subset, providing an independent assessment of end-to-end accuracy. Results are reported in Section 5.2.2.

## 5 Experiments and Results

### 5.1 Pre-Deployment Evaluation

Before full-scale deployment, we conduct a comprehensive evaluation of COMPASS to validate its accuracy on marine Pb data integration. We present detailed experimental analyses aimed at addressing the following three research questions (**RQs**):

- **RQ1:** Can COMPASS accurately integrate target marine Pb data, and how does it compare with general-purpose LLMs?
- **RQ2:** What are the advantages of COMPASS over domain-specific fine-tuned LLMs in terms of performance and cost?
- **RQ3:** How does each core component contribute to overall performance?

**5.1.1 Experimental Setup.** We define the evaluation task, describe the benchmark dataset, and specify the metrics for evaluation.

**Task Overview.** To evaluate whether COMPASS can accurately perform scientific data integration, we structure the evaluation into three core experimental tasks. This stepwise design mirrors the typical workflow used by researchers:

- *Paper Classification:* Identify whether a given paper belongs to the specific subfield relevant to the data integration task.
- *Table Classification:* Identify whether a specific table within a paper includes target data for extraction.
- *End-to-End Extraction:* Extract all target data points from the entire paper collection.

**Table 1: Categories of academic papers in the marine Pb benchmark dataset.**

Category	Description
Marine Pb conc.	Papers reporting dissolved or particulate Pb concentrations in marine environments.
Marine <sup>210</sup> Pb	Papers reporting <sup>210</sup> Pb concentrations in marine environments.
Marine Pb isotopes ratios	Papers reporting Pb isotope ratios (e.g., <sup>206</sup> Pb/ <sup>204</sup> Pb) in marine environments.
Marine Pb (non-target)	Papers containing marine Pb data irrelevant to target tasks (negative control).
Atmospheric Pb	Papers focusing on atmospheric Pb sources and deposition processes.
Terrestrial Pb	Papers focusing on Pb in terrestrial systems (soils, freshwater, etc.).
Analytical Pb	Papers on laboratory methods and analytical techniques for Pb analysis.
Irrelevant “Pb”	Papers mentioning “Pb” but unrelated to lead or environmental science.
Other marine elements	Papers on marine geochemistry of elements other than Pb.
Unrelated topics	Papers completely unrelated to Pb research or marine science.

**Benchmark Dataset.** To evaluate extraction performance, we construct a benchmark dataset distributed across 10 categories (Table 1). “Marine Pb”, “Atmospheric Pb”, and “Terrestrial Pb” are used for the Paper Classification task, as these reflect key environmental compartments relevant to Pb research. Within Marine Pb, we distinguish three target subcategories—Marine Pb conc., Marine <sup>210</sup>Pb, and Marine Pb isotope ratios—whose associated tables provide the target data for table classification and end-to-end data extraction tasks. Tables containing target marine Pb data serve as positive examples, while tables from the remaining seven categories act as negative controls to assess classification robustness. We curated a total of 337 tables, among which 63 contain target marine Pb data, yielding 1,397 data points for downstream extraction tasks.

**Metrics and Configuration.** We employ accuracy (Acc), precision (Prec), recall (Rec), and F1-score for comprehensive quantitative evaluation. All models use greedy decoding (temperature=0) for deterministic and reproducible results. Open-source LLMs are loaded with 4-bit NF4 quantization (BitsAndBytes) with fp16 inference. Maximum generation length is set to 32 tokens for classification and 2,048 tokens for extraction tasks. All experiments are conducted on two NVIDIA RTX 3090 GPUs (24GB VRAM each).

**Baselines.** As there are no agent-based approaches for scientific data integration, we compare COMPASS with two categories of baselines. *General-purpose LLMs:* GPT-4o, Gemini-2.5-pro, Llama-3.1-8B-Instruct, Qwen3-8B, and Qwen2.5-32B-Instruct, representing state-of-the-art proprietary and open-source models. *Domain-specific LLMs:* K2 [11], a Llama-based model pretrained on geoscience data (limited to 2,048-token context), and OceanGPT [6] (Qwen2-7B-based), fine-tuned on ocean science data. To ensure fairness, all baselines are evaluated using identical, iteratively refined prompts (available in our repository).

**5.1.2 Results and Analysis. Overall Performance (RQ1).** As shown in Table 2, COMPASS achieves the highest scores across all tasks,

**Table 2: Performance comparison on the marine Pb benchmark.**

Model	Size	Paper Classification		Table Classification		End-to-End Extraction		
		Acc	F1	Acc	F1	Prec	Rec	F1
GPT-4o	N/A	0.930	0.845	0.778	0.688	0.429	0.330	0.373
Gemini-2.5-pro	N/A	0.960	0.913	0.724	0.681	0.334	<b>0.511</b>	0.404
K2 (LLaMA)	7B	0.050	0.037	0.000	0.000	0.000	0.000	0.000
OceanGPT	7B	0.800	0.748	0.312	0.385	0.038	0.005	0.009
Llama-3.1	8B	0.820	0.757	0.691	0.613	0.067	0.085	0.075
Qwen3	8B	0.880	0.801	0.769	0.658	0.175	0.223	0.196
Qwen2.5	32B	0.920	0.887	0.766	0.684	0.320	0.394	0.353
COMPASS (Ours)	8B	0.960	0.942	<b>0.947</b>	<b>0.897</b>	0.196	0.158	0.175
	32B	<b>0.960</b>	<b>0.956</b>	0.920	0.865	<b>0.508</b>	0.429	<b>0.465</b>

exceeding 90% accuracy in both classification tasks. In end-to-end extraction, COMPASS (32B) achieves 0.465 F1, outperforming GPT-4o (0.373) and Gemini-2.5-pro (0.404). The advantage is most pronounced in table classification, where Knowledge Tree guidance enables accurate distinction between target Pb tables and scientifically irrelevant ones. While Gemini-2.5-pro achieves higher recall (0.511 vs. 0.429), its substantially lower precision (0.334 vs. 0.508) reflects a tradeoff unsuitable for scientific database construction, where data integrity is paramount.

**Advantages over Fine-tuned Models (RQ2).** Domain-specific models perform poorly despite their domain training: K2 fails due to context length limitations, while OceanGPT achieves only 0.009 F1 in extraction. Fine-tuning enhances domain vocabulary but degrades the instruction-following capabilities essential for multi-step integration. COMPASS preserves these capabilities while injecting expertise through the Knowledge Tree, avoiding costly retraining.

**Ablation Study (RQ3).** Table 3 shows that removing tree structured logic reduces end-to-end F1 from 0.465 to 0.402, while removing knowledge nodes reduces it to 0.381. The tree structure ensures systematic task decomposition, while expert knowledge enables scientifically grounded decisions—their combination yields synergistic improvements. The higher recall but lower precision of the ablated variant reflects a precision–recall tradeoff: less structured extraction recovers more records at the cost of data integrity. Enabling automated validation rollback—which directly exercises the Validation Criteria (VC) dimension—further improves end-to-end F1 to 0.619, demonstrating VC’s contribution to overall reliability. Rollback results are reported here rather than in Table 2, as baselines are evaluated under single-pass extraction for fair comparison.

## 5.2 Deployment Results

We deploy COMPASS with the Qwen2.5-32B backbone for full-scale marine Pb data integration, selected for its open-source nature and favorable performance-cost balance.

**5.2.1 Integration Overview.** We retrieve over 230,000 open-access papers using Pb-related keywords. COMPASS hierarchically processes these papers and identifies 110 containing target marine Pb data, extracting 3,751 new records. Combined with 12,704 records from 46 public datasets and 19,108 records from GEOTRACES [3], the integration yields a total of 35,563 marine Pb records.

**Table 3: Ablation study of COMPASS (Qwen2.5-32B backbone). “+rollback” activates the full pipeline with automated validation rollback, directly exercising the Validation Criteria (VC) knowledge dimension.**

Model	Paper Classification		Table Classification		End-to-End Extraction		
	Acc	F1	Acc	F1	Prec	Rec	F1
Qwen2.5-32B (vanilla)	0.920	0.887	0.766	0.684	0.320	0.394	0.353
w/o tree-structured logic	0.940	0.944	0.864	0.800	0.364	0.449	0.402
w/o knowledge nodes	0.950	0.907	0.896	0.825	0.382	0.380	0.381
COMPASS (Ours)	0.960	0.956	0.920	0.865	0.508	0.429	0.465
COMPASS + rollback	<b>0.960</b>	<b>0.956</b>	<b>0.920</b>	<b>0.865</b>	<b>0.750</b>	<b>0.526</b>	<b>0.619</b>

Compared to the 19,108 records in GEOTRACES—the most authoritative existing data product—our effort introduces 16,455 new records, representing an 86% increase in available data. We categorize all records into eight types: Pb concentration,  $^{210}\text{Pb}$  concentration, and six isotope ratios ( $^{206}\text{Pb}/^{204}\text{Pb}$ ,  $^{207}\text{Pb}/^{204}\text{Pb}$ ,  $^{208}\text{Pb}/^{204}\text{Pb}$ ,  $^{206}\text{Pb}/^{207}\text{Pb}$ ,  $^{208}\text{Pb}/^{206}\text{Pb}$ ,  $^{208}\text{Pb}/^{207}\text{Pb}$ ). As shown in Figure 2, this significantly enhances global coverage, particularly in previously undersampled regions such as the East China Sea, Arabian Sea, and Southern Ocean. The complete source paper list is in Appendix A. On benchmark papers containing target data, COMPASS achieves an average per-paper recall of 0.745, offering a practical proxy for within-paper extraction completeness.

The full pipeline required approximately 52 GPU hours on dual RTX 3090 GPUs, an efficiency improvement of over four orders of magnitude compared to manual curation [32]. The one-time Knowledge Tree construction cost is detailed in Section 4.3.

### 5.2.2 Data Quality Assessment. Automated Constraint Checks.

All 3,751 extracted records are validated against physical constraints encoded in the Knowledge Tree’s Validation Criteria. Value range verification and geographical boundary checks achieved 100% pass rates, while unit conversion validation reached 95%. Records that failed automated checks were flagged, rolled back, and re-processed by COMPASS. Rollback was triggered in approximately 0.06% of processed cases across the full 230,000-paper corpus, with each instance limited to re-processing a single step, resulting in negligible additional computational overhead.

**Expert Manual Validation.** We conducted stratified sampling across the 110 identified papers, reviewing 22 papers (20%): 12 Pb conc., 4  $^{210}\text{Pb}$  conc., 5 Pb isotopes ratios, and 1 mixed. These 22 papers yielded 946 data points, of which 869 were confirmed correct, giving 92% accuracy (95% CI:  $\pm 1.7\%$ ). The review was led by one marine scientist with a second providing overall consistency checks. Of the 77 erroneous data points ( $\sim 8\%$ ), errors stem primarily from semantic confusion (43,  $\sim 56\%$ ), e.g., rainwater samples collected during marine cruises misclassified as seawater, or sediment data confused with dissolved-phase measurements; followed by data association errors (26,  $\sim 34\%$ ), e.g., mismatched latitude/longitude or depth across tables; and PDF parsing failures (8,  $\sim 10\%$ ), e.g., row misalignment in upstream parsing. Note that Table 2 reports single-pass extraction for fair baseline comparison; with rollback enabled, COMPASS achieves F1: 0.619 (see Table 3). The remaining gap with the 92% deployment accuracy stems from two factors:

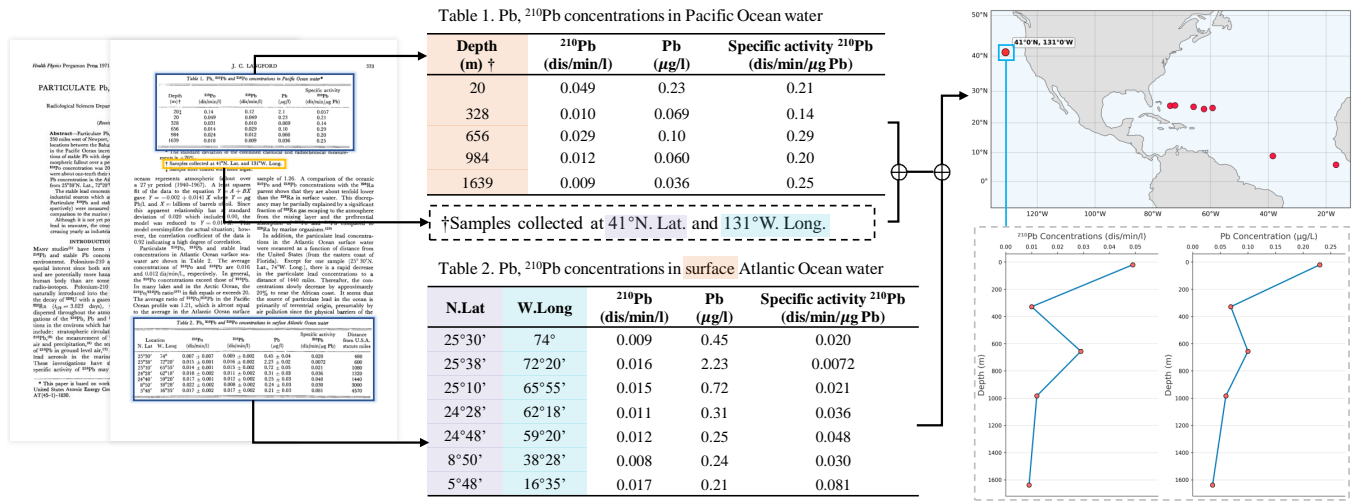


**Figure 6: Case study of COMPASS data integration. COMPASS identifies relevant data tables, associates Pb measurements with metadata (coordinates from footnotes, depth from captions) within each table, and consolidates records into a unified dataset. Data sourced from Langford (1971) [25].**

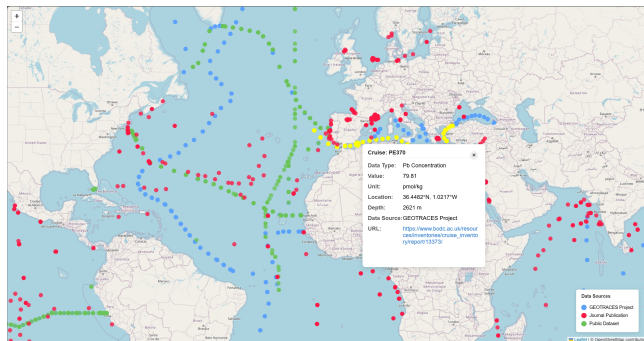


**Figure 7: Screenshot of the online platform providing interactive spatial visualization, cruise-based data viewing, data querying, and source traceability.**

the benchmark penalizes unextracted data regardless of paper relevance, and expert validation accepts minor coordinate variants (e.g., degree-minute conversions) that automated metrics penalize.

**5.2.3 Case Study.** Figure 6 illustrates the COMPASS workflow in Langford (1971) [25]. COMPASS identifies two relevant data tables and performs intra-table data association for each: in the first table, Pb measurements are linked with geographic coordinates recorded in its footnotes; in the second, data values are associated with the depth information specified in its caption. The independently resolved records from both tables are then consolidated into a unified, standardized dataset.

**5.3 Online Data Platform**

We launch an interactive online platform<sup>3</sup> integrated into the open-source JingWei marine data system for visualization and exploration

<sup>3</sup>https://jingwei.acemap.cn/lead

of the Pb database. Users can query records with full metadata and source provenance (Figure 7). Since launch, the platform has received over 1,590 visits, demonstrating its practical utility for marine scientific research.

**5.4 Scientific Insights**

The integrated marine Pb database provides a substantially enriched data landscape compared to existing resources, enabling scientific analyses previously infeasible due to data limitations.

**Enhanced Global Coverage.** As shown in Figure 2, the integrated database extends spatial coverage across all eight Pb measurement types. Among the 3,751 newly extracted records, concentration measurements constitute the largest share, with 1,228 Pb concentration and 472 <sup>210</sup>Pb activity concentration records that directly support global Pb inventory estimation and vertical flux studies. The three <sup>204</sup>Pb-normalized isotope ratios (<sup>206</sup>Pb/<sup>204</sup>Pb: 562; <sup>207</sup>Pb/<sup>204</sup>Pb: 532; <sup>208</sup>Pb/<sup>204</sup>Pb: 476) provide the most diagnostic power for source apportionment, as <sup>204</sup>Pb is the only non-radiogenic stable Pb isotope. Additional paired ratios (<sup>206</sup>Pb/<sup>207</sup>Pb: 246; <sup>208</sup>Pb/<sup>206</sup>Pb: 139; <sup>208</sup>Pb/<sup>207</sup>Pb: 96), though fewer in number, complement source identification in regions where <sup>204</sup>Pb measurements are unavailable. This broader coverage reduces reliance on interpolation for global Pb budget estimation, particularly in the Southern Hemisphere and marginal seas.

**Regional Data Enrichment.** The integration reveals previously under-sampled patterns in several key regions. In the *East China Sea*, newly incorporated Pb concentration and isotope data capture the influence of Yangtze River discharge and East Asian industrial emissions, filling a critical gap in global databases for this highly impacted marginal sea. In the *Southern Ocean*, recovered records from historical expedition reports provide valuable constraints on pre-industrial Pb baselines and the penetration of anthropogenic Pb

into deep waters. In the *Arabian Sea*, new records complement GEO-TRACES transects by adding temporal depth, enabling investigation of how regional Pb sources have evolved over decades.

**Implications for Anthropogenic Impact Assessment.** The temporal span of the dataset—from the 1960s to the present—enables multi-decadal trend analysis. The global phase-out of leaded gasoline provides a natural experiment for studying oceanic recovery, and our data capture both the peak contamination and recovery phases across diverse regions. The comprehensive isotope coverage supports source apportionment, linking observed Pb patterns to anthropogenic emissions. These insights demonstrate that systematically recovering scattered historical records enables a more complete understanding of human impacts on ocean chemistry.

## 6 Conclusion

In this paper, we propose COMPASS, a Knowledge Tree-enhanced LLM Agent framework that operationalizes an expert-guided adaptation approach for fine-grained scientific data integration from academic papers. By co-designing a domain-specific Knowledge Tree with marine scientists, COMPASS bridges the gap between general-purpose LLMs and high-stakes scientific domains without fine-tuning. Deploying COMPASS across over 230,000 open-access papers, we recover 3,751 previously unincorporated Pb records, substantially expanding the integrated marine Pb database, with 92% accuracy confirmed through expert validation. The newly integrated data reveal previously obscured patterns in under-sampled regions such as the East China Sea and the Southern Ocean. In the future, we plan to extend COMPASS to additional scientific domains and integrate multi-modal processing capabilities.

## 7 Limitations and Ethical Considerations

Despite COMPASS's effectiveness, we acknowledge certain limitations delineating our current scope. Our implementation focuses on extracting data from tables and text, excluding figures. This is a strategic choice: the vast majority of marine Pb records are reported in tabular or textual format, whereas graphical representations are less commonly used for data reporting in this domain. Furthermore, extraction quality is partially bounded by upstream PDF parsing tools. While layout recognition errors can propagate through the pipeline, our modular design ensures that COMPASS will naturally benefit from future advancements in general document analysis. Finally, the Knowledge Tree requires expert-guided initialization; while this incurs a setup cost, the construction process is iterative and accumulates reusable experience—including core module design and structural patterns—such that subsequent updates or generalization to other scientific domains primarily require domain-specific knowledge adaptation rather than rebuilding the entire framework from scratch.

**Ethical Considerations.** All data are sourced from publicly available open-access papers with no personally identifiable information. Our platform ensures transparency by linking every integrated record to its original source to support reproducibility.

## 8 GenAI Disclosure

During the preparation of this manuscript, generative AI tools were used to assist with language refinement and grammatical

correction of certain draft passages. All scientific contributions, including methodology, experiments, analysis and conclusions, are solely the work of the authors.

## Acknowledgments

This work was supported by National Natural Science Foundation of China (No. T2421002, 62602003, 62272293), Postdoctoral Fellowship Program of CPSF under Grant No. GZB20250806, and the AI for Science Seed Program of Shanghai Jiao Tong University (project number 2025AI4S-QY01).

## References

- [1] Maya Almaraz, Chao Wang, and Michelle Y Wong. 2025. Deep soil contributions to global nitrogen budgets. *Nature Communications* 16, 1 (2025), 966.
- [2] Waleed Ammar, Dirk Groeneveld, Chandra Bhagavatula, Iz Beltagy, Miles Crawford, Doug Downey, Jason Dunkelberger, Ahmed Elgohary, Sergey Feldman, Vu Ha, Rodney Kinney, Sebastian Kohlmeier, Kyle Lo, Tyler Murray, Hsu-Han Ooi, Matthew E. Peters, Joanna Power, Sam Skjonsberg, Lucy Lu Wang, Chris Wilhelm, Zheng Yuan, Madeleine van Zuylen, and Oren Etzioni. 2018. Construction of the Literature Graph in Semantic Scholar. In *Proceedings of the 2018 Conference of the North American Chapter of the Association for Computational Linguistics: Human Language Technologies, NAACL-HLT 2018, New Orleans, Louisiana, USA, June 1-6, 2018, Volume 3 (Industry Papers)*. Association for Computational Linguistics, 84–91.
- [3] Robert F Anderson. 2020. GEOTRACES: Accelerating research on the marine biogeochemical cycles of trace elements and their isotopes. *Annual Review of Marine Science* 12, 1 (2020), 49–85.
- [4] Adib Bazgir, Yuwen Zhang, et al. 2025. Multicrossmodal Automated Agent for Integrating Diverse Materials Science Data. *arXiv preprint arXiv:2505.15132* (2025).
- [5] Iz Beltagy, Kyle Lo, and Arman Cohan. 2019. SciBERT: A Pretrained Language Model for Scientific Text. In *Proceedings of the 2019 Conference on Empirical Methods in Natural Language Processing and the 9th International Joint Conference on Natural Language Processing (EMNLP-IJCNLP)*, Kentaro Inui, Jing Jiang, Vincent Ng, and Xiaojun Wan (Eds.). Association for Computational Linguistics, Hong Kong, China, 3615–3620. doi:10.18653/v1/D19-1371
- [6] Zhen Bi, Ningyu Zhang, Yida Xue, Yixin Ou, Daxiong Ji, Guozhou Zheng, and Huajun Chen. 2024. OceanGPT: A Large Language Model for Ocean Science Tasks. In *Proceedings of the 62nd Annual Meeting of the Association for Computational Linguistics (Volume 1: Long Papers)*, Lun-Wei Ku, Andre Martins, and Vivek Srikumar (Eds.). Association for Computational Linguistics, Bangkok, Thailand, 3357–3372. doi:10.18653/v1/2024.acl-long.184
- [7] Edward A Boyle, Jong-Mi Lee, Yolanda Echehoven, Abigail Noble, Simone Moos, Gonzalo Carrasco, Ning Zhao, Richard Kayser, Jing Zhang, Toshitaka Gamo, et al. 2014. Anthropogenic lead emissions in the ocean: The evolving global experiment. *Oceanography* 27, 1 (2014), 69–75.
- [8] Hengxing Cai, Xiaochen Cai, Shuwen Yang, Jiankun Wang, Lin Yao, Zhifeng Gao, Junhan Chang, Sihang Li, Mingjun Xu, Changxin Wang, et al. 2024. Uni-SMART: Universal Science Multimodal Analysis and Research Transformer. *arXiv preprint arXiv:2403.10301* (2024).
- [9] Daniel J Cziczko, Olaf Stetzer, Annette Worringer, Martin Ebert, Stephan Weinbruch, Michael Kamphus, Stephane J Gallavardin, Joachim Curtius, Stephan Borrmann, Karl D Froyd, et al. 2009. Inadvertent climate modification due to anthropogenic lead. *Nature geoscience* 2, 5 (2009), 333–336.
- [10] John Dagdelen, Alexander Dunn, Sanghoon Lee, Nicholas Walker, Andrew S Rosen, Gerbrand Ceder, Kristin A Persson, and Anubhav Jain. 2024. Structured information extraction from scientific text with large language models. *Nature Communications* 15, 1 (2024), 1418.
- [11] Cheng Deng, Tianhang Zhang, Zhongmou He, Qiyuan Chen, Yuanyuan Shi, Yi Xu, Luoyi Fu, Weinan Zhang, Xinbing Wang, Chenghu Zhou, et al. 2024. K2: A foundation language model for geoscience knowledge understanding and utilization. In *Proceedings of the 17th ACM International Conference on Web Search and Data Mining*. 161–170.
- [12] Jun-xuan Fan, Shu-zhong Shen, Douglas H Erwin, Peter M Sadler, Norman MacLeod, Qiu-ming Cheng, Xu-dong Hou, Jiao Yang, Xiang-dong Wang, Yue Wang, et al. 2020. A high-resolution summary of Cambrian to Early Triassic marine invertebrate biodiversity. *Science* 367, 6475 (2020), 272–277.
- [13] Yuchen Fang, Zhenggang Tang, Kan Ren, Weiqing Liu, Li Zhao, Jiang Bian, Dongsheng Li, Weinan Zhang, Yong Yu, and Tie-Yan Liu. 2023. Learning Multi-Agent Intention-Aware Communication for Optimal Multi-Order Execution in Finance. In *Proceedings of the 29th ACM SIGKDD Conference on Knowledge Discovery and Data Mining (Long Beach, CA, USA) (KDD '23)*. Association for Computing Machinery, New York, NY, USA, 4003–4012. doi:10.1145/3580305.3599856

- [14] Alireza Ghafarollahi and Markus J. Buehler. 2025. SciAgents: Automating Scientific Discovery Through Bioinspired Multi-Agent Intelligent Graph Reasoning. *Advanced Materials* 37, 22 (2025), 2413523. arXiv:https://advanced.onlinelibrary.wiley.com/doi/pdf/10.1002/adma.202413523 doi:10.1002/adma.202413523
- [15] Alex Griffiths, Hollie Packman, Yee-Lap Leung, Barry J Coles, Katharina Kreissig, Susan H Little, Tina van de Fliedert, and Mark Rehkaemper. 2020. Evaluation of optimized procedures for high-precision lead isotope analyses of seawater by multiple collector inductively coupled plasma mass spectrometry. *Analytical Chemistry* 92, 16 (2020), 11232–11241.
- [16] Yue Guo, Wentao Zhang, Xiaojun Zhang, Vincent W. Zheng, and Yi Yang. 2025. Efficient Multi-Expert Tabular Language Model for Banking. In *Proceedings of the 31st ACM SIGKDD Conference on Knowledge Discovery and Data Mining V.1* (Toronto ON, Canada) (KDD '25). Association for Computing Machinery, New York, NY, USA, 2271–2281. doi:10.1145/3690624.3709400
- [17] Qianyue Hao, Wenzhen Huang, Tao Feng, Jian Yuan, and Yong Li. 2023. GAT-MF: Graph Attention Mean Field for Very Large Scale Multi-Agent Reinforcement Learning. In *Proceedings of the 29th ACM SIGKDD Conference on Knowledge Discovery and Data Mining* (Long Beach, CA, USA) (KDD '23). Association for Computing Machinery, New York, NY, USA, 685–697. doi:10.1145/3580305.3599359
- [18] Gideon M. Henderson and Ernst Maier-Reimer. 2002. Advection and removal of 210Pb and stable Pb isotopes in the oceans: a general circulation model study. *Geochimica et Cosmochimica Acta* 66, 2 (2002), 257–272. doi:10.1016/S0016-7037(01)00779-7
- [19] Mengkang Hu, Pu Zhao, Can Xu, Qingfeng Sun, Jian-Guang Lou, Qingwei Lin, Ping Luo, and Saravan Rajmohan. 2025. AgentGen: Enhancing Planning Abilities for Large Language Model based Agent via Environment and Task Generation. In *Proceedings of the 31st ACM SIGKDD Conference on Knowledge Discovery and Data Mining V.1* (Toronto ON, Canada) (KDD '25). Association for Computing Machinery, New York, NY, USA, 496–507. doi:10.1145/3690624.3709321
- [20] Earl B Hunt, Janet Marin, and Philip J Stone. 1966. Experiments in induction. (1966).
- [21] Song Jiang, Zijie Huang, Xiao Luo, and Yizhou Sun. 2023. CF-GODE: Continuous-Time Causal Inference for Multi-Agent Dynamical Systems. In *Proceedings of the 29th ACM SIGKDD Conference on Knowledge Discovery and Data Mining* (Long Beach, CA, USA) (KDD '23). Association for Computing Machinery, New York, NY, USA, 997–1009. doi:10.1145/3580305.3599272
- [22] Ghazal Khalighinejad, Sharon Scott, Ollie Liu, Kelly L. Anderson, Rickard Stureborg, Aman Tyagi, and Bhuwan Dhingra. 2025. MatViX: Multimodal Information Extraction from Visually Rich Articles. In *Proceedings of the 2025 Conference of the Nations of the Americas Chapter of the Association for Computational Linguistics: Human Language Technologies (Volume 1: Long Papers)*, Luis Chiruzzo, Alan Ritter, and Lu Wang (Eds.). Association for Computational Linguistics, Albuquerque, New Mexico, 3636–3655. doi:10.18653/v1/2025.naacl-long.185
- [23] Hanyu Lai, Xiao Liu, Jat Long Long, Shuntian Yao, Yuxuan Chen, Pengbo Shen, Hao Yu, Hanchen Zhang, Xiaohan Zhang, Yuxiao Dong, et al. 2024. AutoWebGLM: A Large Language Model-based Web Navigating Agent. In *Proceedings of the 30th ACM SIGKDD Conference on Knowledge Discovery and Data Mining*, 5295–5306.
- [24] Jakub Lála, Odhran O'Donoghue, Aleksandar Shtedritski, Sam Cox, Samuel G Rodrigues, and Andrew D White. 2023. Paperqa: Retrieval-augmented generative agent for scientific research. *arXiv preprint arXiv:2312.07559* (2023).
- [25] J. C. Langford. 1971. Particulate Pb, 210Pb and 210Po in the Environment. *Health Physics* 20, 3 (March 1971), 331–336.
- [26] Patrick Lewis, Ethan Perez, Aleksandra Piktus, Fabio Petroni, Vladimir Karpukhin, Naman Goyal, Heinrich Küttler, Mike Lewis, Wen-tau Yih, Tim Rocktäschel, et al. 2020. Retrieval-augmented generation for knowledge-intensive nlp tasks. *Advances in neural information processing systems* 33 (2020), 9459–9474.
- [27] Xin Li, Feng Liu, Chunfeng Ma, Jinliang Hou, Donghai Zheng, Hanqing Ma, Yulong Bai, Xujun Han, Harry Vereecken, Kun Yang, et al. 2024. Land data assimilation: Harmonizing theory and data in land surface process studies. *Reviews of Geophysics* 62, 1 (2024), e2022RG000801.
- [28] Xin Li, Hanqing Ma, Youhua Ran, Xufeng Wang, Gaofeng Zhu, Feng Liu, Honglin He, Zhen Zhang, and Chunlin Huang. 2021. Terrestrial carbon cycle model-data fusion: Progress and challenges. *Science China Earth Sciences* 64, 10 (2021), 1645–1657.
- [29] Jana Lipkova, Richard J Chen, Bowen Chen, Ming Y Lu, Matteo Barbieri, Daniel Shao, Anurag J Vaidya, Chengkuan Chen, Luoting Zhuang, Drew FK Williamson, et al. 2022. Artificial intelligence for multimodal data integration in oncology. *Cancer cell* 40, 10 (2022), 1095–1110.
- [30] Yuxuan Liu, Hongda Sun, Wei Liu, Jian Luan, Bo Du, and Rui Yan. 2025. MobileSteward: Integrating Multiple App-Oriented Agents with Self-Evolution to Automate Cross-App Instructions. In *Proceedings of the 31st ACM SIGKDD Conference on Knowledge Discovery and Data Mining V.1* (Toronto ON, Canada) (KDD '25). Association for Computing Machinery, New York, NY, USA, 883–893. doi:10.1145/3690624.3709171
- [31] Jerome O Nriagu and Jozef M Pacyna. 1988. Quantitative assessment of worldwide contamination of air, water and soils by trace metals. *nature* 333, 6169 (1988), 134–139.
- [32] B. Nussbaumer-Streit, M. Ellen, I. Klerings, R. Sfetcu, N. Riva, M. Mahmić-Kaknjo, G. Poulentzas, P. Martinez, E. Baladia, L.E. Ziganashina, M.E. Marqués, L. Aguilár, A.P. Kassianos, G. Frampton, A.G. Silva, L. Affengruber, R. Spjker, J. Thomas, R.C. Berg, M. Kontogianni, M. Sousa, C. Kontogiorgis, and G. Gartlehner. 2021. Resource use during systematic review production varies widely: a scoping review. *Journal of Clinical Epidemiology* 139 (2021), 287–296. doi:10.1016/j.jclinepi.2021.05.019
- [33] Clair C Patterson. 1965. Contaminated and natural lead environments of man. *Archives of Environmental Health: An International Journal* 11, 3 (1965), 344–360.
- [34] Bernhard K. Schaule and Clair C. Patterson. 1981. Lead concentrations in the northeast Pacific: evidence for global anthropogenic perturbations. *Earth and Planetary Science Letters* 54, 1 (1981), 97–116. doi:10.1016/0012-821X(81)90072-8
- [35] Xiangru Tang, Tianyu Hu, Muyang Ye, Yanjun Shao, Xunjian Yin, Siru Ouyang, Wangchunshu Zhou, Pan Lu, Zhuosheng Zhang, Yilun Zhao, et al. 2025. Chemaqent: Self-updating memories in large language models improves chemical reasoning. In *The Thirteenth International Conference on Learning Representations*.
- [36] Omkarprasad S Vaidya and Sushil Kumar. 2006. Analytic hierarchy process: An overview of applications. *European Journal of operational research* 169, 1 (2006), 1–29.
- [37] Bin Wang, Chao Xu, Xiaomeng Zhao, Linke Ouyang, Fan Wu, Zhiyuan Zhao, Rui Xu, Kaiwen Liu, Yuan Qu, Fukai Shang, Bo Zhang, Liqun Wei, Zhihao Sai, Wei Li, Botian Shi, Yu Qiao, Dahua Lin, and Conghui He. 2024. MinerU: An Open-Source Solution for Precise Document Content Extraction. arXiv:2409.18839 [cs.CV] https://arxiv.org/abs/2409.18839
- [38] Jingwei Wang, Qianyue Hao, Wenzhen Huang, Xiaochen Fan, Qin Zhang, Zhen-tao Tang, Bin Wang, Jianye Hao, and Yong Li. 2025. CoopRide: Cooperate All Grids in City-Scale Ride-Hailing Dispatching with Multi-Agent Reinforcement Learning. In *Proceedings of the 31st ACM SIGKDD Conference on Knowledge Discovery and Data Mining V.1* (Toronto ON, Canada) (KDD '25). Association for Computing Machinery, New York, NY, USA, 1457–1468. doi:10.1145/3690624.3709205
- [39] Xinbing Wang, Luoyi Fu, Xiaoying Gan, Ying Wen, Guanjie Zheng, Jiaxin Ding, Liyao Xiang, Nanyang Ye, Meng Jin, Shiyu Liang, Bin Lu, Haiwen Wang, Yi Xu, Cheng Deng, Shao Zhang, Huquan Kang, Xingli Wang, Qi Li, Zhixin Guo, Jiexing Qi, Pan Liu, Yuyang Ren, Lyuwen Wu, Jungang Yang, Jianping Zhou, and Chenghu Zhou. 2024. AceMap: Knowledge Discovery through Academic Graph. *CoRR abs/2403.02576* (2024).
- [40] Xumeng Wen, Han Zhang, Shun Zheng, Wei Xu, and Jiang Bian. 2024. From Supervised to Generative: A Novel Paradigm for Tabular Deep Learning with Large Language Models. In *Proceedings of the 30th ACM SIGKDD Conference on Knowledge Discovery and Data Mining* (Barcelona, Spain) (KDD '24). Association for Computing Machinery, New York, NY, USA, 3323–3333. doi:10.1145/3637528.3671975
- [41] Jingfeng Wu and Edward A Boyle. 1997. Lead in the western North Atlantic Ocean: Completed response to leaded gasoline phaseout. *Geochimica et Cosmochimica Acta* 61, 15 (1997), 3279–3283. doi:10.1016/S0016-7037(97)89711-6
- [42] Mingzhe Xing, Hangyu Mao, Shenglin Yin, Lichen Pan, Zhengchao Zhang, Zhen Xiao, and Jieyi Long. 2023. A Dual-Agent Scheduler for Distributed Deep Learning Jobs on Public Cloud via Reinforcement Learning. In *Proceedings of the 29th ACM SIGKDD Conference on Knowledge Discovery and Data Mining* (Long Beach, CA, USA) (KDD '23). Association for Computing Machinery, New York, NY, USA, 2776–2788. doi:10.1145/3580305.3599241
- [43] Hancheng Zhang, Guozheng Li, Chi Harold Liu, Guoren Wang, and Jian Tang. 2023. HiMacMic: Hierarchical Multi-Agent Deep Reinforcement Learning with Dynamic Asynchronous Macro Strategy. In *Proceedings of the 29th ACM SIGKDD Conference on Knowledge Discovery and Data Mining* (Long Beach, CA, USA) (KDD '23). Association for Computing Machinery, New York, NY, USA, 3239–3248. doi:10.1145/3580305.3599379
- [44] J. Zhang, Z.T. Ni, J.L. Ren, F. Yu, X.Y. Diao, Y. Wang, S.J. Zhang, H. Su, S.L. Cong, Z.J. Lu, S. Jiang, J. Ou, Y. Chen, Q. Wang, Z.B. Zhang, J.T. Ai, C.B. Wang, and Z.D. Tao. 2024. Modular ocean trace elements sampling for the international GEOTRACES studies – Evidence from analysis of dissolved Fe and Pb. *Progress in Oceanography* 221 (2024), 103212. doi:10.1016/j.pocean.2024.103212
- [45] Weichao Zhao, Hao Feng, Qi Liu, Jingqun Tang, Binghong Wu, Lei Liao, Shu Wei, Yongjie Ye, Hao Liu, Wengang Zhou, et al. 2024. Tabpedia: Towards comprehensive visual table understanding with concept synergy. *Advances in Neural Information Processing Systems* 37 (2024), 7185–7212.
- [46] Cheryl M Zurbrick, Céline Gallon, and A Russell Flegal. 2017. Historic and industrial lead within the Northwest Pacific Ocean evidenced by lead isotopes in seawater. *Environmental Science & Technology* 51, 3 (2017), 1203–1212.

## A Complete Paper List

Table 4 presents the complete list of 110 papers that were identified by COMPASS during its deployment in marine Pb data integration.

**Table 4: Complete list of papers identified by COMPASS for marine Pb data integration.**

No.	Title	DOI
1	210Pb and 226Ra distributions in the Circumpolar waters	10.1016/0012-821x(81)90100-x
2	210Pb as a tracer of shelf–basin transport and sediment focusing in the Chukchi Sea	10.1016/j.dsr2.2008.10.021
3	210Pb sedimentation rates from the Northwestern Mediterranean margin	10.1016/j.margeo.2005.02.020
4	210Pb-derived chronology and the fluxes of 210Pb and 137Cs isotopes into continental shelf sediments, East Chukchi Sea, Alaskan Arctic	10.1016/0016-7037(95)00248-x
5	210Pb/226Ra and 210Po/210Pb disequilibria in seawater and suspended particulate matter	10.1016/0012-821x(76)90068-6
6	210Pb/226Ra disequilibrium in the Santa Barbara Basin	10.1016/0012-821x(75)90057-6
7	210Pb/226Ra: Radioactive disequilibrium in the deep sea	10.1016/0012-821x(73)90194-5
8	226Ra and 210Pb in the Weddell Sea	10.1016/0012-821x(80)90082-5
9	226Ra, 210Pb and 210Po disequilibria in the Western North Pacific	10.1016/0012-821x(76)90071-6
10	238U decay series nuclides in the northeastern Arabian Sea: Scavenging rates and cycling processes	10.1016/0278-4343(94)90015-9
11	210Pb and 210Po in the equatorial Pacific and the Bering Sea: the effects of biological productivity and boundary scavenging	10.1016/s0967-0645(97)00024-6
12	<sup>210</sup>Pb–<sup>226</sup>Ra–<sup>230</sup>Th systematics in very low sedimentation rate sediments from the Mendeleev Ridge (Arctic Ocean) This article is one of a series of papers published in this Special Issue on the theme–<i>Polar Climate Stability Network</i>–. GEOTOP Publication 2008-0031.	10.1139/e08-047
13	A Voltammetric Study on Toxic Metals, their Speciation and Interaction with Nutrients and Organic Ligand in a South Pacific Ocean Region	10.1080/03067319808026847
14	A comparison of the non-essential elements cadmium, mercury, and lead found in fish and sediment from Alaska and California	10.1016/j.scitotenv.2004.07.028
15	A lead isotopic study of circum-antarctic manganese nodules	10.1016/0016-7037(95)00084-d
16	Accumulation and potential sources of lead in marine organisms from coastal ecosystems of the Chilean Patagonia and Antarctic Peninsula area	10.1016/j.marpolbul.2019.01.026
17	Accumulation of heavy metals (Pb, Zn, Cu, Cd), carbon and nitrogen in sediments from Strait of Georgia, B.C., Canada	10.1016/0304-4203(91)90017-q
18	Analysis of 210Pb in sediment trap samples and sediments from the northern Arabian Sea: evidence for boundary scavenging	10.1016/s0967-0637(02)00013-4
19	Antarctic Marine Sediments: Distribution of Elements and Textural Characters	10.1006/mchj.1998.1586
20	Arctic vs. North Atlantic water mass exchanges in Fram Strait from Pb isotopes in sediments This article is one of a series of papers published in this Special Issue on the theme –<i>Polar Climate Stability Network</i>–.	10.1139/e08-050
21	Assessment of element concentrations in surface sediment samples from Sigacik Bay (eastern Aegean)	10.3906/yer-2002-15
22	Basin-scale seawater lead isotopic character and its geological evolution indicated by Fe–Mn deposits in the SCS	10.1080/1064119x.2019.1637978
23	Bioturbation in the abyssal Arabian Sea: influence of fauna and food supply	10.1016/s0967-0645(00)00052-7
24	Brachidontes variabilis and Patella sp. as quantitative biological indicators for cadmium, lead and mercury in the Lebanese coastal waters	10.1016/j.envpol.2005.09.016
25	Cadmium, copper and lead contamination of the seawater column on the Prestige shipwreck (NE Atlantic Ocean)	10.1016/s0003-2670(04)00333-2
26	Cadmium, copper and lead contamination of the seawater column on the Prestige shipwreck (NE Atlantic Ocean)	10.1016/j.aca.2004.03.032
27	Changes in sediment source areas to the Amerasia Basin, Arctic Ocean, over the past 5.5 million years based on radiogenic isotopes (Sr, Nd, Pb) of detritus from ferromanganese crusts	10.1016/j.margeo.2020.106280
28	Colloid/Solution Partitioning of Metal-Selective Organic Ligands, and its Relevance to Cu, Pb and Cd Cycling in the Firth of Clyde	10.1006/ecss.1997.0267
29	Comparative Base Line Studies on Pb-Levels in European Coastal Waters	10.1016/b978-0-08-022960-7.50017-8
30	Comparative studies on trace metal levels in marine biota	10.1007/bf01359516
31	Concentration and isotopic composition of dissolved Pb in surface waters of the modern global ocean	10.1016/j.gca.2018.05.005
32	Concentration profiles of barium and lead in Atlantic waters off Bermuda	10.1016/0012-821x(66)90035-5
33	Concentrations of Cu and Pb in the offshore and intertidal sediments of the west coast of Peninsular Malaysia	10.1016/s0160-4120(02)00073-9
34	Datierung von Ostseesedimenten mit<sup>210</sup>Pb	10.1080/10256019008624336
35	Deposition rates, mixing intensity and organic content in two contrasting submarine canyons	10.1016/j.pocan.2008.01.001
36	Determination of lead isotope ratios in seawater by quadrupole inductively coupled plasma mass spectrometry after Mg(OH)2 co-precipitation	10.1016/s0584-8547(00)00176-2
37	Determination of mass accumulation rates and sediment radionuclide inventories in the deep Black Sea	10.1016/0967-0637(94)90064-7
38	Differing controls over the Cenozoic Pb and Nd isotope evolution of deepwater in the central North Pacific Ocean	10.1016/j.epsl.2004.12.009
39	Dissolved trace metals in the surface waters of Puget Sound	10.1016/0025-326x(85)90568-5
40	Distribution of dissolved and particulate 226Ra, 210Pb and 210Po in the Bismarck Sea and western equatorial Pacific Ocean	10.1071/mf99170
41	Do decreased trace metal concentrations in surficial skagerrak sediments over the last 15–30 years indicate decreased pollution?	10.1016/0269-7491(94)90132-5
42	Effects of bottom water dissolved oxygen variability on copper and lead fractionation in the sediments across the oxygen minimum zone, western continental margin of India	10.1016/j.scitotenv.2016.05.125
43	Enrichment in Trace Metals (Al, Mn, Co, Cu, Mo, Cd, Fe, Zn, Pb and Hg) of Macro-Invertebrate Habitats at Hydrothermal Vents Along the Mid-Atlantic Ridge	10.1007/s10750-005-4758-1
44	Evaluation of the use of common sculpin (Myoxocephalus scorpius) organ histology as bioindicator for element exposure in the fjord of the mining area Maarmorilik, West Greenland	10.1016/j.envres.2014.05.031
45	Fe–Si–oxyhydroxide deposits at a slow-spreading centre with thickened oceanic crust: The Lilliput hydrothermal field (9°33'S, Mid-Atlantic Ridge)	10.1016/j.chemgeo.2010.09.012
46	Geographic control on Pb isotope distribution and sources in Indian Ocean Fe–Mn deposits	10.1016/s0016-7037(01)00713-x
47	Global environmental effects of large volcanic eruptions on ocean chemistry: Evidence from “hydrothermal” sediments (ODP Leg 185, Site 1149B)	10.1029/2007jb005333
48	Gulf of Guinea continental slope and Congo (Zaire) deep-sea fan: Sr–Pb isotopic constraints on sediments provenance from ZaiAngo cores	10.1016/j.margeo.2005.11.014
49	Heavy metal pollution and its relation to the malformation of green mussels cultured in Muara Kamal waters, Jakarta Bay, Indonesia	10.1016/j.marpolbul.2018.06.029
50	Heavy metal sedimentation in Saanich Inlet measured with<sup>210</sup>Pb technique	10.1029/jc082i034p05477
51	Heavy metals from Kueishantao shallow-sea hydrothermal vents, offshore northeast Taiwan	10.1016/j.jmarsys.2016.11.018
52	High-precision measurements of seawater Pb isotope compositions by double spike thermal ionization mass spectrometry	10.1016/j.aca.2014.12.012
53	Hydrothermal Fe–Si–Mn oxide deposits from the Central and South Valu Fa Ridge, Lau Basin	10.1016/j.apgeochem.2011.04.008

Table 4 (cont.)

No.	Title	DOI
54	Implications of excess 210Pb and 137Cs in sediment cores from Mikawa Bay, Japan	10.1016/s1001-0742(08)62328-1
55	Intercomparison of alpha and gamma spectrometry techniques used in 210Pb geochronology	10.1016/j.jenvrad.2006.11.007
56	In-situ enrichment of heavy metals from deep-sea water by an ion-exchange pump system	10.1080/10641199609388319
57	Isotopic analysis of metalliferous sediment from the East Pacific Rise	10.1016/0012-821x(71)90121-x
58	Isotopic evidence for the source of lead in the North Pacific abyssal water	10.1016/j.gca.2010.05.017
59	Isotopic tracing of anthropogenic Pb inventories and sedimentary fluxes in the Gulf of Lions (NW Mediterranean sea)	10.1016/s0278-4343(98)00070-3
60	Late Quaternary variability of Mediterranean Outflow Water from radiogenic Nd and Pb isotopes	10.1016/j.quascirev.2010.06.021
61	Lead in the western North Atlantic Ocean: Completed response to leaded gasoline phaseout	10.1016/s0016-7037(97)89711-6
62	Lead in tropical marine systems: A review	10.1016/0048-9697(86)90071-9
63	Lead isotopic composition of metalliferous sediments from the Nazca plate	10.1130/mem154-p199
64	Lead isotopic disequilibria between plankton assemblages and surface waters reflect life cycle strategies of coastal populations within a northeast Pacific upwelling regime	10.4319/lo.1993.38.3.0670
65	Lead-210 and polonium-210 in the surface water of the Pacific	10.2343/geochemj.5.165
66	Levels of radionuclide concentrations in benthic invertebrate species from the Balearic Islands, Western Mediterranean, during 2012–2018	10.1016/j.marpolbul.2019.110519
67	Marine sediment contamination and dynamics at the mouth of a contaminated torrent: The case of the Gromolo Torrent (Sestri Levante, north-western Italy)	10.1016/j.marpolbul.2016.06.010
68	Mineralogy, geochemistry, and Sr-Pb isotopic geochemistry of hydrothermal massive sulfides from the 15.2°S hydrothermal field, Mid-Atlantic Ridge	10.1016/j.jmarsys.2017.02.010
69	Mixing of particles and organic constituents in sediments from the continental shelf and slope off Cape Cod: SEEP-I results	10.1016/0278-4343(88)90082-9
70	Monthly variation of trace metals in North Sea sediments. From experimental data to modeling calculations	10.1016/j.marpolbul.2014.07.053
71	Natural rates of sediment containment of PAH, PCB and metal inventories in Sydney Harbour, Nova Scotia	10.1016/j.scitotenv.2009.05.029
72	Neoglacial change in deep water exchange and increase of sea-ice transport through eastern Fram Strait: evidence from radiogenic isotopes	10.1016/j.quascirev.2013.06.015
73	New constraints on the Pb and Nd isotopic evolution of NE Atlantic water masses	10.1029/2007gc001766
74	On the role of colloids in trace metal solid-solution partitioning in continental shelf waters: a comparison of model results and field data	10.1016/0278-4343(95)98840-7
75	Particle fluxes and recent sediment accumulation on the Aquitanian margin of Bay of Biscay	10.1016/j.csr.2008.11.018
76	Particle mixing rates in sediments of the eastern equatorial Pacific: Evidence from 210Pb, 239,240Pu and 137Cs distributions at MANOP sites	10.1016/0016-7037(85)90010-9
77	Particulate Pb, 210Pb and 210Po in the Environment	10.1097/00004032-197103000-00011
78	Particulate and dissolved 210Pb activities in the shelf and slope regions of the Gulf of Mexico waters	10.1016/s0278-4343(02)00017-1
79	Patella vulgata, Mytilus minimus and Hyale prevosti as bioindicators for Pb and Se Enrichment in Alexandria coastal waters	10.1016/0025-326x(91)90184-t
80	Pb isotope compositions of modern deep sea turbidites	10.1016/s0012-821x(00)00340-x
81	Pb, Sr, and Nd isotopes in basalts and sulfides from the Juan de Fuca Ridge	10.1029/jb092ib11p11380
82	Pb's high sedimentation inside the bay mouth of Jiaozhou Bay	10.1088/1755-1315/100/1/012071
83	Pollution history of heavy metals on the Portuguese shelf using 210Pb-geochronology	10.1016/j.scitotenv.2006.03.042
84	Recent sedimentation and mass accumulation rates based on 210Pb along the Peru–Chile continental margin	10.1016/j.dsr2.2004.08.015
85	Records of Holocene climatic fluctuations and anthropogenic lead input in elemental distribution and radiogenic isotopes (Nd and Pb) in sediments of the Gulf of Lions (Southern France)	10.1177/0959683619846973
86	Residence times of surface water and particle-reactive 210Pb and 210Po in the East China and Yellow seas	10.1016/0016-7037(91)90305-o
87	SWASV speciation of Cd, Pb and Cu for the determination of seawater contamination in the area of the Nicole shipwreck (Ancona coast, Central Adriatic Sea)	10.1016/j.marpolbul.2011.08.047
88	Seawater quality assessment and identification of pollution sources along the central coastal area of Gabes Gulf (SE Tunisia): Evidence of industrial impact and implications for marine environment protection	10.1016/j.marpolbul.2017.12.012
89	Sediment and organic carbon focusing in the Shelikof Strait, Alaska	10.1016/j.margeo.2005.06.036
90	Sedimentary signals of the upwelling along the Zhejiang coast, China	10.1016/j.ecss.2019.106396
91	Sedimentation of natural radionuclides on the seabed across the northern Japan Trench.	10.2343/geochemj.30.217
92	Settling fluxes of U- and Th-series nuclides in the Bay of Bengal: results from time-series sediment trap studies	10.1016/s0967-0637(00)00016-9
93	Some features of the trace metal biogeochemistry in the deep-sea hydrothermal vent fields (Menez Gwen, Rainbow, Broken Spur at the MAR and 9°50'N at the EPR): A synthesis	10.1016/j.jmarsys.2012.09.005
94	Source and distribution of lead in the surface sediments from the South China Sea as derived from Pb isotopes	10.1016/j.marpolbul.2010.07.026
95	Spatial and temporal distribution of Fe, Ni, Cu and Pb along 140°E in the Southern Ocean during austral summer 2001/02	10.1016/j.marchem.2008.05.001
96	Spatial and temporal distribution of heavy metals in coastal core sediments from the Red Sea, Saudi Arabia	10.1080/03067319.2017.1317762
97	Strontium, lead and zinc isotopes in marine cores as tracers of sedimentary provenance: A case study around Taiwan orogen	10.1016/j.chemgeo.2007.10.024
98	Sub-part per trillion levels of lead and isotopic profiles in a fjord, using an ultra-clean pumping system	10.1016/s0304-4203(99)00070-5
99	Sulfur and lead isotopic compositions of massive sulfides from deep-sea hydrothermal systems: Implications for ore genesis and fluid circulation	10.1016/j.oregeorev.2016.10.014
100	The behaviour of 210Pb and 226Ra in the eastern Irish Sea	10.1016/0265-931x(90)90025-q
101	The distribution of lead concentrations and isotope compositions in the eastern Tropical Atlantic Ocean	10.1016/j.gca.2018.01.018
102	The use of Pb-210 geochronology as a sedimentological tool: Application to the Washington continental shelf	10.1016/0025-3227(79)90039-2
103	Trace elements in surface sediments from Kongsfjorden, Svalbard: occurrence, sources and bioavailability	10.1080/03067319.2017.1317762
104	Trace metal variability, background levels and pollution status assessment in line with the water framework and Marine Strategy Framework EU Directives in the waters of a heavily impacted Mediterranean Gulf	10.1016/j.marpolbul.2014.07.054
105	Trace metals (Co, Ni, Cu, Cd, and Pb) in the southern East/Japan Sea	10.1007/s12601-014-0006-9
106	Trace metals in Antarctic copepods from the Weddell Sea (Antarctica)	10.1016/s0045-6535(02)00855-x
107	Tracing the source of Pb using stable Pb isotope ratios in sediments of eastern Beibu Gulf, South China Sea	10.1016/j.marpolbul.2019.02.028
108	Unusual ratios in the surface water of the Gulf of Lions	10.1016/s0399-1784(98)80030-3
109	Vertical distribution of 210Pb and 226Ra and their activity ratio in marine sediment core of the East Malaysia coastal waters	10.1007/s10967-011-1206-8
110	What controls the mixed-layer depth in deep-sea sediments? The importance of POC flux	10.4319/lo.2002.47.2.0418